Proceedings of the IASS 2024 Symposium
Redefining the Art of Structural Design
August 26-30, 2024, Zurich Switzerland
Philippe Block, Giulia Boller, Catherine DeWolf,
Jacqueline Pauli, Walter Kaufmann (eds.)

An innovative hollow-cable dome for indoor cooling application

Yongcan DONG[a], Shu LI[a,*], Xingfei YUAN[a,*], Zhendong QIU[a], Akram SAMY[b]

[a,*] College of Civil Engineering and Architecture, Zhejiang University
Hangzhou, China
*lishu99@zju.edu.cn
*yuanxf@zju.edu.cn

[b] College of Civil Engineering, Xinjiang University

Abstract

Considering the space requirement of long-span spatial structure and the requirement of its internal comfort, an innovative hollow-cable dome structure is proposed in this paper. Through the substitution of conventional cables with flexible pipes, the configuration characteristic of continuous cables allows for the formation of a continuous volume within the structure. When the cold air flows in and circulates internally, the hollow-cable dome can function as an air conditioning pipe system, allowing for the adjustment of indoor temperature. Accordingly, the proposed structure realizes dual functions of structural bearing and temperature adjustment. The thermal-fluid analysis framework for hollow-cable dome is proposed in this paper. Additionally, to verify the feasibility and practicability of the structure and its function, the heat transfer process and indoor cooling process are simulated and analyzed in Fluent, demonstrating a valuable application prospect. Furthermore, this paper also explores factors affecting the indoor cooling efficiency, providing a basis for further optimizing the design of the hollow-cable dome structure.

Keywords: cable dome, thermal analysis, hydraulic analysis, structural bearing capacity, cooling simulation

1. The innovative hollow-cable-strut system

On the basis of cable dome structure configuration, through replacing conventional cables with flexible hollow pipes, an innovative hollow-cable dome is formed accordingly. With a Levy hollow-cable dome as the illustrative example, as shown in Figure 1. It's apparent that a continuous pipe network is formed in the structure, similar to the air conditioning pipe system.

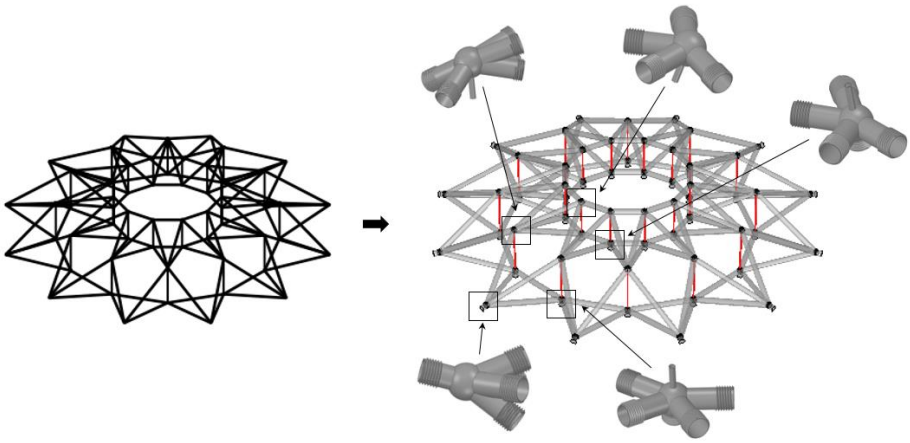

Figure 1: Structural design of innovative hollow-cable dome

The configuration of hollow nodes is significant, and typical nodes are highlighted in Figure 1(a). All nodes can be further classified into three types: inlet node, outlet node, and internal node. Generally, the index of inlet and outlet nodes can be designated arbitrarily. This paper assumes that nodes on the outer ring beam of the cable dome are all inlet nodes, connecting guide pipes, and bottom end nodes of each layer vertical struts are all outlet nodes, whose guide pipes are convenient for the outflow of air. Taking an outlet node as an example, Figure 2 illustrates its configuration and the connective strategy of hollow nodes with hollow cables and struts. The threads on guide pipes of hollow nodes are configured for convenient connections.

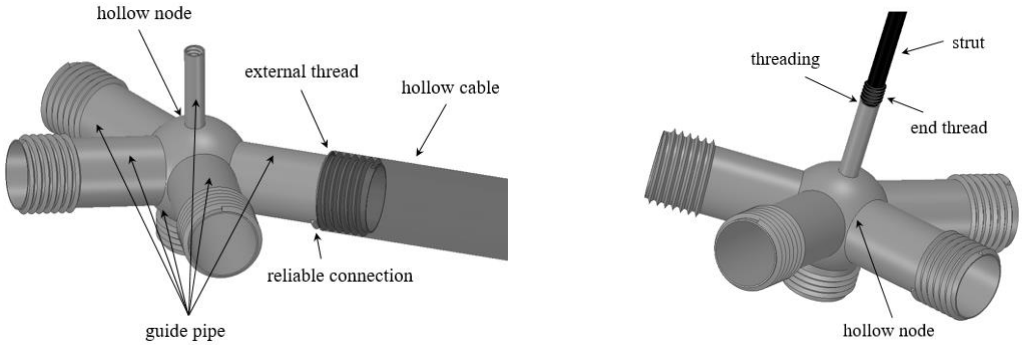

(a) Connection between cable and hollow node (b) Connection between strut and hollow node

Figure 2: Connective strategy of elements and nodes

Considering the input of cold air into the hollow-cable dome structure, the cold air can flow into the structure through the rationally arranged outlets and then circulate in the inner space for indoor cooling. Consequently, the proposed hollow-cable dome structure can achieve dual functions of structural load bearing and temperature regulation, so as to effectively alleviate the problems of complex design of air conditioning pipes, material consumption and space occupation. At the same time, it conforms to the green and low-carbon sustainable design concept.

2. Structural analysis and thermal analysis

2.1. Structural analysis

For a structure with n_n nodes and n_e elements, the node coordinate vector $\boldsymbol{n} \in \boldsymbol{R}^{3n_\mathrm{n}}$, describing the configuration of a tensegrity structure, is as follows:

$$\boldsymbol{n} = [\boldsymbol{n}_1{}^\mathrm{T}, \boldsymbol{n}_2{}^\mathrm{T}, \cdots, \boldsymbol{n}_{n_\mathrm{n}}{}^\mathrm{T}]^\mathrm{T} \tag{1}$$

The connection matrix $\boldsymbol{C} \in \boldsymbol{R}^{n_\mathrm{e} \times n_\mathrm{n}}$ is applied to illustrate the connection relationship between elements and nodes of the structure. For an element *i* connected by node *j* and *k*, the *j*th and *k*th entries of the *i*th row of matrix $\boldsymbol{C}$ are -1 and 1, respectively, and other entries are all 0. And in order to conduct the static calculation of the structure, the static equilibrium equation is established [1]:

$$\boldsymbol{K}\boldsymbol{n} = \boldsymbol{w} \tag{2}$$

in which $\boldsymbol{K}$ is the global stiffness matrix. The tangent stiffness matrix $\boldsymbol{K}_\mathrm{T}$ can be obtained by taking the first derivation of $\boldsymbol{K}\boldsymbol{n}$ with respect to $\boldsymbol{n}$, which can be further written as the sum of the geometric stiffness $\boldsymbol{K}_\mathrm{G}$ and the material stiffness $\boldsymbol{K}_\mathrm{E}$:

$$\boldsymbol{K}_\mathrm{T} = \boldsymbol{K}_\mathrm{G} + \boldsymbol{K}_\mathrm{E} \tag{3}$$

where $\boldsymbol{K}_\mathrm{G}$ and $\boldsymbol{K}_\mathrm{E}$ can be calculated through

$$\boldsymbol{K}_\mathrm{G} = (\boldsymbol{C}^\mathrm{T}\hat{\boldsymbol{q}}\boldsymbol{C}) \otimes \boldsymbol{I}_3 \tag{4}$$

$$\boldsymbol{K}_\mathrm{E} = \boldsymbol{A}_1\hat{\boldsymbol{E}}\hat{\boldsymbol{A}}\hat{\boldsymbol{l}}^{-3}\boldsymbol{A}_1^\mathrm{T} \tag{5}$$

2.2. Thermal-fluid analysis

For ease of calculation, several assumptions are made first: a) the fluid pressure load are concentrated on structural nodes; b) the thermal effect is exerted on the structure through the overall cooling field; c) the most unfavorable case of fluid pressure loads and temperature loads are considered.

The fluid pressure load f_{f}, acing on the node along the axial direction, and the structural thermal stress σ_{T} caused by the temperature change can be calculated through

$$f_{\mathrm{f}} = p_{\max} A_{\mathrm{s}} \tag{6}$$

$$\sigma_{\mathrm{T}} = \alpha \Delta T E \tag{7}$$

in which $p_{\max}$ is the maximum fluid pressure within the structure, and A_{s} is the cross-sectional area of the pipe. α is the linear expansion coefficient of the material, ΔT is the temperature change and E represents the elastic modulus of the material.

Considering the normal load situation, and simultaneously considering the heat flow effect on the hollow-cable dome, the fluid load $\boldsymbol{F}_{\mathrm{f}}$ and temperature load $\boldsymbol{F}_{\mathrm{t}}$ are combined into $\boldsymbol{W}_{\mathrm{total}}$, the load matrix. Then the static analysis of hollow-cable dome structure under thermal-fluid loads is carried out.

$$\boldsymbol{K}\boldsymbol{n} = \boldsymbol{W}_{\mathrm{total}} \tag{8}$$

The analysis framework of the hollow-cable dome under thermal-fluid loads is established with reference to the partitioned solution of fluid-structure interaction [2], as illustrated in Figure 3.

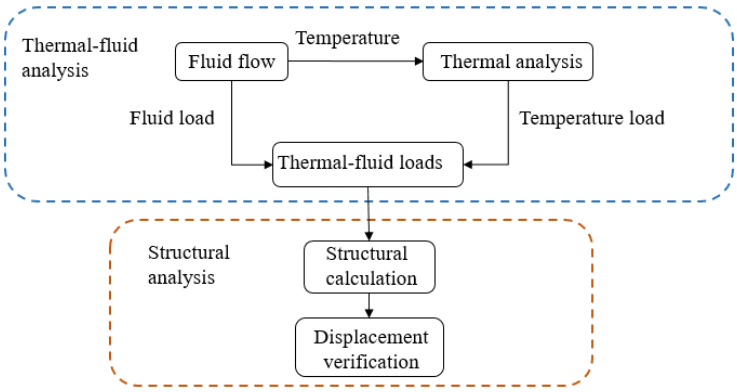

Figure 3: Analysis framework

3. Numerical examples

In this section, numerical examples of hollow-cable dome structures are simulated and analyzed, so as to explore the feasibility and effectiveness of the structure for indoor cooling, and further investigate factors affecting its cooling efficiency. The simulation analysis of the hollow-cable dome includes the heat flow simulation within the structure, the structural FEM simulation and the indoor cooling simulation. Accordingly, the joint simulation analysis of Fluent-APDL is considered, and the specific simulation process is shown in Figure 4.

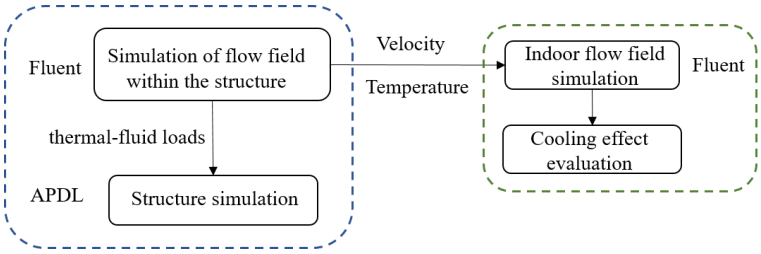

Figure 4: Simulation process

3.1. Example establishment

Four examples are proposed to analyze, as shown in Figure 5. Example-A, a Levy hollow-cable dome with inner ring, is discussed and analyzed in detail as the reference. Then Example-B, -C and -D are established by adjusting the section size of components, the structural complexity and the structural configuration to explore factors affecting the indoor cooling efficiency.

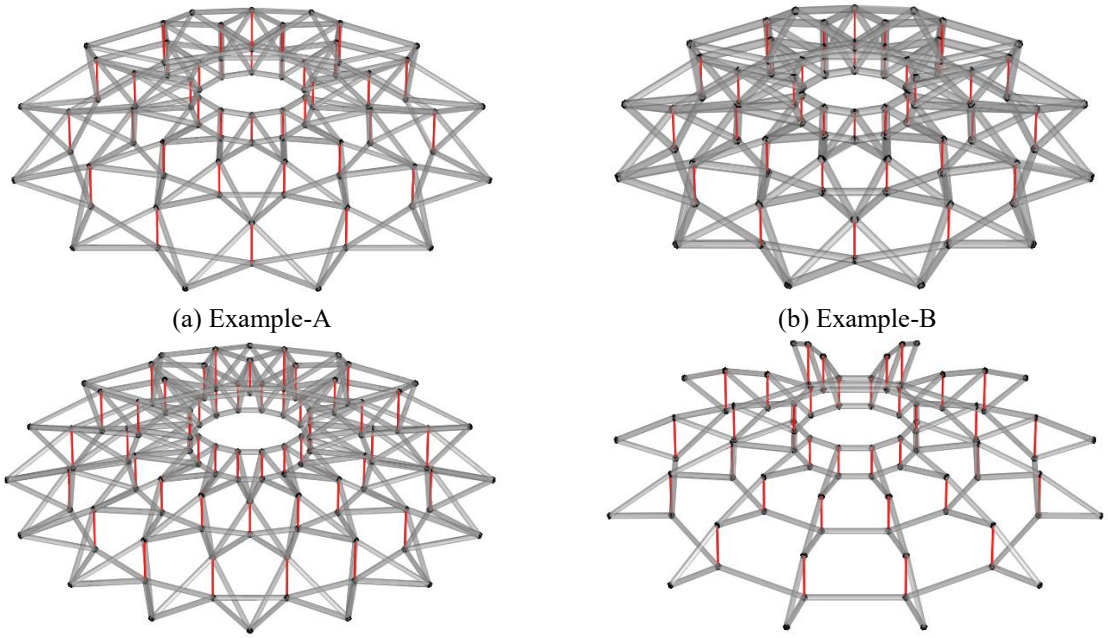

(a) Example-A (b) Example-B

(c) Example-C (d) Example-D

Figure 5: Four examples

3.1.1. ***Example-A***

Example-A is established based on the configuration of a Levy cable dome with inner ring. Considering the symmetry, nodes 1~7 can form a basic unit and there are 12 basic units in the structure, all of which are rotationally symmetric about z-axis. Then coordinates of nodes 1~7 are listed in Table 1, and coordinates of the rest nodes can be obtained accordingly.

Table 1 Node coordinates of a basic unit in Example-A

Element	1	2	3	4	5	6	7
x	-10.8667	-7.5000	-3.6222	-10.8667	-7.5000	-3.6222	-15.0000
y	-2.9117	0.0000	-0.9706	-2.9117	0.0000	-0.9706	0.0000
z	2.3257	3.8485	4.7171	-0.6681	1.3899	2.6947	0.0000

Each basic unit contains 19 components, which can be divided into 13 groups. The prestress mode of Levy cable dome can be obtained though SVD [3]. And when the internal force of inner layer struts G3 is set as 9000 N, the inner forces *t* of all elements in a unit are detailed in Table 2.

Table 2: Internal forces of elements in a basic unit

Element	*t* / N	Element	*t* / N	Element	*t* / N	Element	*t* / N
G1	-1.58×10^5	JS1	1.89×10^5	JS2	4.92×10^4	JS3	2.12×10^4
G2	-3.19×10^4	XS1	6.03×10^5	XS2	7.74×10^4	XS3	1.62×10^4
G3	-9.00×10^3	HS1	1.48×10^6	HS2	2.21×10^5	HS3	5.27×10^4
H0	6.99×10^4						

As for the material, CFRP pipe and Q345B circular steel pipe are selected for tension and compression members respectively. Corresponding material parameters are listed in Table 3. In addition, the insulation material is employed to wrap the CFRP pipe for the reduction of heat loss and maintenance of stable temperature, so as to achieve more accurate temperature control and cooling effect.

Table 3 Material Property

Material	CFRP	Q345B steel tube
Density / (kg/m^3)	1700	7850
Modulus / (N/m^2)	2.30×10^{11}	2.06×10^{11}
Possion's ratio	0.27	0.3
Coefficient of thermal expansion / K^{-1}	2×10^{-6}	1.2×10^{-5}
Specific heat capacity / (J·kg^{-1}·K^{-1})	712	480

In terms of section size, all hollow members are of the same section size in order to guarantee the continualness of the flow and the uniformity and efficiency of the heat transfer, while the load bearing capacity and structural safety should be ensured. φ 170×5 CFRP pipe is applied, whose effective cross-sectional area is taken as its ring area, and all struts are made of φ 63×5 Q345B circular steel pipe

3.1.2. Comparison examples

Based on Example-A, only the change of a single parameter is considered to form the following examples to explore the influence factors of cooling efficiency. However, it should be noted that due to the high correlation of shape and internal forces, considering that the internal force of internal struts is assumed to be 9000 N all the time, when the configuration parameters change, the internal force distribution will also change accordingly. But this only affects the stiffness of the structure, and then affects the displacement of the structure, which will be discussed and analyzed in the future research.

The section size of hollow cables is adjusted to form Example-B, as shown in Figure 5(b). The flexible hollow pipe adopts φ 256×8 CFRP pipe. And seen in Figure 5(c), the complexity of Example-C is changed to 16, while other conditions remain unchanged. In terms of the influence of cable dome configuration on the cooling efficiency, Example-D considers the establishment of a Geiger hollow-cable dome structure with three rings and inner rings, as depicted in Figure 5(d).

3.2. Complete analysis of Example-A

Sub-processes of the complete joint simulation analysis for Example-A are as follows [4].

3.2.1. Thermal-fluid simulation

The thermal-fluid simulation is conducted in Fluent. The inlet velocity of the stadium is taken as 5 m/s according to the general design criteria, and the initial temperature is set as 298 K. Considering the cooling function of the input of cold air, the inlet temperature is set to 278 K. The outlet uses 0 Pa pressure boundary. The wall boundary condition is set to heat flux and the value is 0, that is, the adiabatic wall.

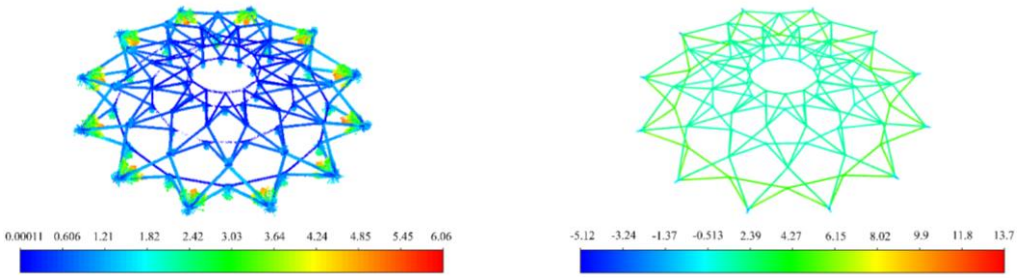

(a) Velocity distribution / (m/s) (b) Temperature distribution / K

Figure 6: Diagram of velocity and temperature distribution

Since the air inside the hollow-cable dome structure is in turbulent flow state, the realizable k-ε turbulent flow calculation model is adopted. In the simulation process, the flow velocity distribution and pressure distribution of the fluid within the structure are shown in Figure 6. According to the simulation result, when stable, the external outlet flow velocity is the highest at 2.40 m/s, while the internal and middle layers have similar outlet flow velocity at 1.28 m/s and 1.32 m/s, respectively, providing initial conditions for the subsequent indoor cooling simulation. Under ideal conditions, cold air reaches outlets of the structure almost without heat loss and the temperature of all outlets is 278 K.

3.2.2. Structural analysis

Considering its normal load condition as well as its thermal-fluid load, the bearing capacity of the hollow-cable dome structure should be calculated and checked. Based on the above heat flow simulation results, the most unfavorable fluid pressure and the temperature load is focused, that is, the maximum node pressure value in the structure and the cooling load of 20 K are taken into consideration. Load combination is carried out according to Load Code [5], and then the loads of nodes on each circle of vertical rods are calculated according to the projected area, which are listed in Table 4. At the same time, 20 K cooling load is applied to the structure according to the overall cooling field. And the static analysis of the proposed structure is carried out in ANSYS.

Table 4: Loads on nodes of each vertical strut / N

	Inner veritical struts	Middle veritical struts	Outer veritical struts
Load	5520	17670	26500

The simulation result shows that the maximum node displacement of the 30m-span Levy hollow-cable dome structure in this example is only 4.7 mm, well meeting the displacement limit requirement in the technical specification [6]. Therefore, the innovative hollow-cable dome structure can maintain its normal structural bearing capacity and use safety while functioning as the pipe system for cold air transportation and indoor cooling.

3.2.3. Indoor cooling simulation

As shown in Figure 7(a), the Levy hollow-cable dome is applied in a stadium with 30 m span, acting as an air conditioning pipe system. And Figure 7(b) depicts the xz-profile of the Levy hollow-cable dome structure and the stadium. The stadium covers an area of about 707 m^2. Fixed nodes of the external ring are all connected with fluid inlets, and bottom nodes of vertical struts are all connected with fluid outlets. Therefore, there are 12 inlets and 36 outlets, whose lengths are all set as 0.5 m. The cold air flows into the interior space through outlets, circulates internally, and then exits through doors (with a width of 1m and a height of 3 m) in four directions of the stadium.

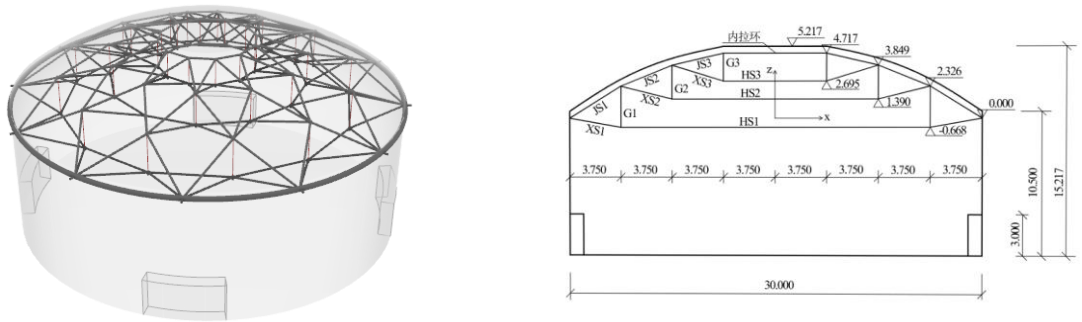

(a) Application scenario (b) *xz*-profile scheme / m

Figure 7: Innovative hollow-cable dome applied in a stadium

Once there is a temperature gradient, heat transfer occurs, which means that the heat energy will flow from the high temperature region to the low temperature region until the temperature equilibrium is

reached. The influence of external environment is ignored, and the adiabatic wall boundary conditions are considered. The heat transfer process of the flow field in the stadium is simulated in Fluent. Through the calculation of 4000s, the temperature of the entire indoor space dropped by about 8 K, showing a significant cooling effect.

3.3. Factors affecting cooling efficiency Simulation analysis and comparison

In order to explore the factors affecting the cooling efficiency of the hollow-cable dome structure, the analyses of other three examples are conducted based on the complete analysis of Example-A. In the heat flow simulation, the results of velocity of outlets from Example-A~D are listed in Table 5, all of which meet the flow conservation.

Table 5: Velocity of outlets / (m/s)

	Example-A	Example-B	Example-C	Example-D
internal outlet	1.28	1.40	1.27	1.10
middle outlet	1.32	1.24	1.42	1.30
external outlet	2.40	2.36	2.31	2.60

Based on velocity results in Table 5, the indoor cooling simulation is conducted when applied to the statidum of the same size. Since the length of vertical strut and the radius of loop cables remain unchanged, the profile dimensions of Example-A~D are completely consistent, as depicted in Figure 7(b). During the cooling simulation process, temperature monitoring is carried out at z=-1 m plane, as shown in Figure 8.

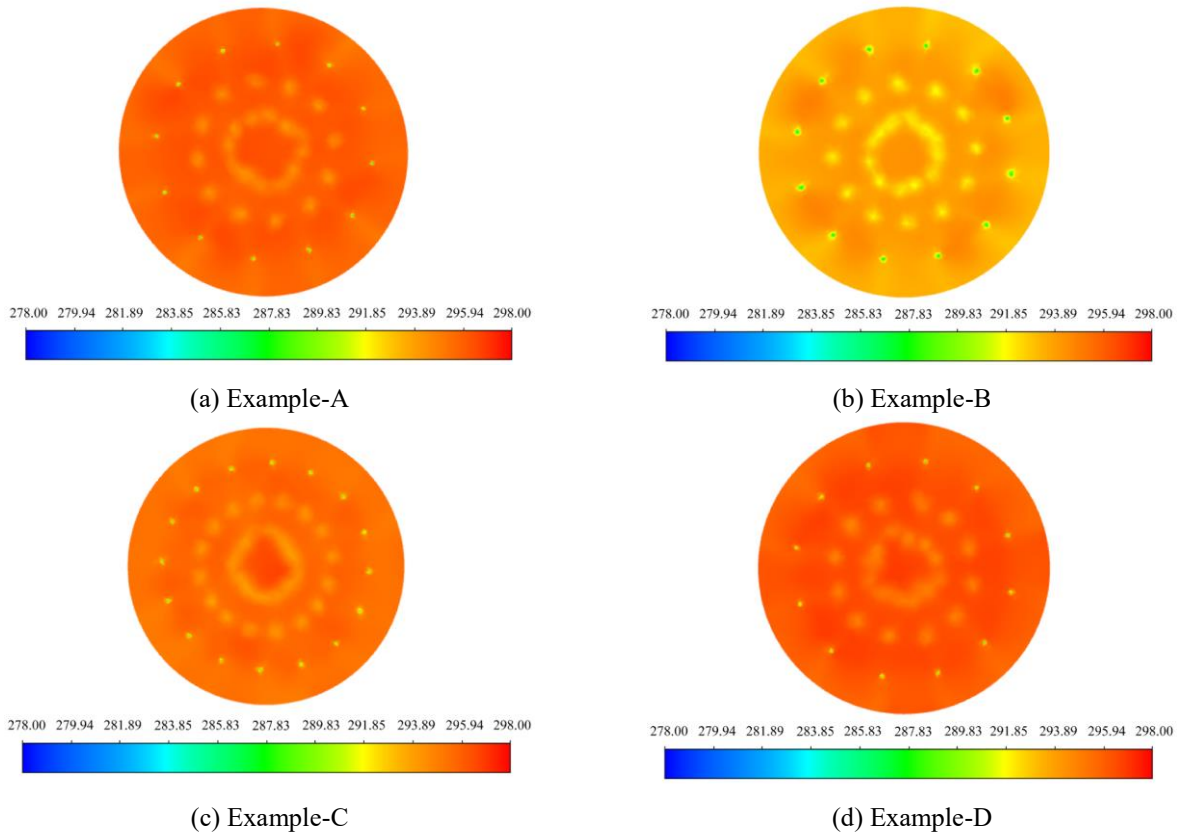

Figure 8: Example-A~D temperature monitoring of z=-1 m plane / K

The average temperatures of Example-A~D at z=-1 m plane after 1000s calculation are listed in Table 6. Taking the temperature change of z=-1 m plane as the evaluation standard of the cooling effect, the

cooling conditions of the four examples are compared. Furthermore, the average temperature curve of z=-1 m plane over time is drawn, as shown in Figure 9.

Table 6: Evaluation of indoor cooling effect

	Example-A	Example-B	Example-C	Example-D
Configuration	Levy	Levy	Levy	Geiger
Complexity	12	12	16	12
Number of outlets	36	36	48	36
Total outlet area / m^2	0.723	1.628	0.965	0.723
Proportion	0.102%	0.230%	0.136%	0.102%
Cooling effect / K	2.10	4.27	2.54	1.80

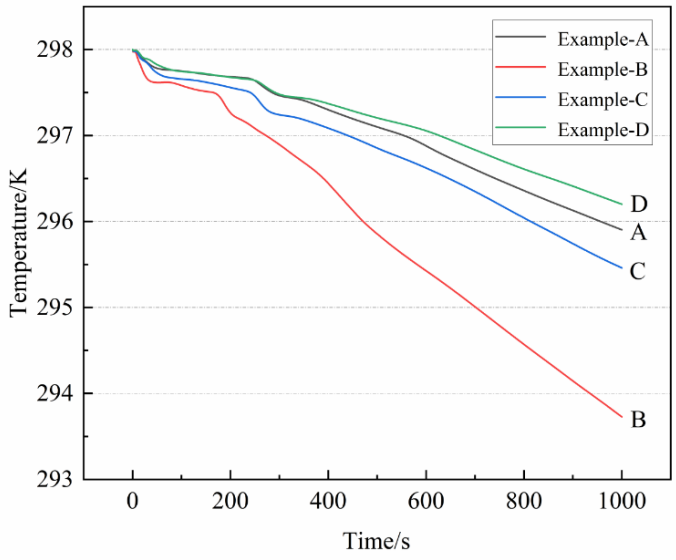

Figure 9: Average temperature variation in z=-1 m plane

We found that, with the cooling effect of Example-A as the reference, Example-D was slightly lower, while Example-B and -C are improved by comparison. Among them, Example-B has the highest cooling efficiency and exibits the most obvious effect. It is apparent that the cooling effect is mainly related to the total outlet area. The component size and the cable dome complexity both affect the area of outlets, thus affecting the cooling effect. In addition, the complexity of the cable dome will affect the uniformity of indoor temperature changes. Compared with Example-C and -A, when the complexity of the cable dome is higher, the indoor temperature changes will be more uniform, so that hot and cold concentration areas can be well avoided. Considering cable dome configurations in Example-D and -A, since the number of cables in Geiger configuration is less than that of Levy configuration, which means that the number of fluid channels in the corresponding hollow-cable dome structure is affected, the outlet velocity is relatively slow and the cooling effect is slightly decreased.

In sum, the indoor cooling effect and efficiency of the proposed hollow-cable dome structure are closely related to the selected component parameters and structural configuration, providing theoretical foundation for the optimization of the structure for better functioning.

4. Conclusion

This paper proposes an innovative hollow-cable dome structure, and focuses on its temperature adjustment application exploration. With flexible hollow pipes acting as tension members, a continuous flow path is formed within the structure, and the hollow-cable dome structure can be regarded as a pipe system, transporting cold air while carrying normal loads as bearing structure. The main conclusions are as follows:

1) The results of joint simulations in Fluent and ANSYS APDL well demonstrate that the proposed hollow-cable dome structure has the integrated function of structural bearing and cold air conveying, which can reduce space occupation and material comsuption.

2) Through reasonable arrangement of outlets, the uniform distribution of cold air in the internal space can be guaranteed and the waste of hot areas and cold air can be avoided. The comfort and energy consumption are well improved, in line with green and sustainable building design concepts.

3) The indoor cooling effect and efficiency of the hollow-cable dome structure are closely related to the structural configuration and component parameters. By optimizing the design parameters of the proposed hollow-cable dome structure, its cooling capacity can be effectively improved.

Acknowledgements

The research was supported by the National Natural Science Foundation of China (Grant No. 52278224), and the Natural Science Foundation of Zhejiang Province (Grant No. Z24E080001).

References

[1] F. K. Benra, H. J. Dohmen, J. Pei, "A Comparison of One-Way and Two-Way Coupling Methods for Numerical Analysis of Fluid-Structure Interactions", *Journal of Applied Mathematics*, 2011.

[2] S. Ma, M. H. Chen, and R. E. Skelton, "Tensegrity system dynamics based on finite element method", *Composite Structures*, vol. 280, 2022.

[3] S. Pellegrino, "Structural computations with the singular value decomposition of the equilibrium matrix", *International Journal of Space Structures*, vol. 30, no. 21, pp. 3025-3035, 1993.

[4] S. Li, X. Yuan, A. Samy, "Study on innovative hollow-cable domes for indoor cooling", *Spatial Structures*, Accepted, 2024. (in Chinese)

[5] Ministry of Housing and Urban-Rural Development, *Load Code for the design of building structures GB 50009—2012*, China Building Industry Press, 2012.

[6] Ministry of Housing and Urban-Rural Development, *Technical specification for cable structures JGJ 257-2012*, China Building Industry Press, 2012.